**Atmospheric
Measurement
Techniques**

Detection of HO_2 by laser-induced fluorescence: calibration and interferences from RO_2 radicals

H. Fuchs, B. Bohn, A. Hofzumahaus, F. Holland, K. D. Lu, S. Nehr, F. Rohrer, and A. Wahner

Institute of Energy and Climate Research: Troposphere (IEK-8), Forschungszentrum Jülich GmbH, Jülich, Germany

Abstract. HO_2 concentration measurements are widely accomplished by chemical conversion of HO_2 to OH including reaction with NO and subsequent detection of OH by laser-induced fluorescence. RO_2 radicals can be converted to OH via a similar radical reaction sequence including reaction with NO, so that they are potential interferences for HO_2 measurements. Here, the conversion efficiency of various RO_2 species to HO_2 is investigated. Experiments were conducted with a radical source that produces OH and HO_2 by water photolysis at 185 nm, which is frequently used for calibration of LIF instruments. The ratio of HO_2 and the sum of OH and HO_2 concentrations provided by the radical source was investigated and was found to be 0.50 ± 0.02. RO_2 radicals are produced by the reaction of various organic compounds with OH in the radical source. Interferences via chemical conversion from RO_2 radicals produced by the reaction of OH with methane and ethane (H-atom abstraction) are negligible consistent with measurements in the past. However, RO_2 radicals from OH plus alkene- and aromatic-precursors including isoprene (mainly OH-addition) are detected with a relative sensitivity larger than 80 % with respect to that for HO_2 for the configuration of the instrument with which it was operated during field campaigns. Also RO_2 from OH plus methyl vinyl ketone and methacrolein exhibit a relative detection sensitivity of 60 %. Thus, previous measurements of HO_2 radical concentrations with this instrument were biased in the presence of high RO_2 radical concentrations from isoprene, alkenes or aromatics, but were not affected by interferences in remote clean environment with no significant emissions of biogenic VOCs, when the OH reactivity was dominated by small alkanes. By reducing the NO concentration and/or the transport time between NO addition and OH detection, interference from these RO_2 species are suppressed to values below 20 % relative to the HO_2 detection sensitivity. The HO_2 conversion efficiency is also smaller by a factor of four, but this is still sufficient for atmospheric HO_2 concentration measurements for a wide range of conditions.

1 Introduction

The measurement of hydroperoxy radical (HO_2) concentrations is important for the understanding of the photochemical degradation of atmospheric trace gases and the formation of secondary air pollutants such as ozone (e.g., Finlayson-Pitts and Pitts Jr., 2000). HO_2 is mainly produced by radical chain reactions, starting with the reaction of CO or volatile organic compounds (VOC) with photochemically produced hydroxyl radicals (OH). It is also formed by the photolysis of carbonyl compounds, ozonolysis and the reaction of the nitrate radical (NO_3) with organic compounds (e.g., Geyer et al., 2003; Kanaya et al., 2007).

Because of the small radical concentrations in the atmosphere within the range of some ten parts per trillion per volume (pptv) (e.g. Monks, 2005; Kanaya et al., 2007; Lelieveld et al., 2008; Hofzumahaus et al., 2009) high instrument sensitivities are required for the detection of HO_2. Matrix Isolation Electron Spin Resonance Spectroscopy (MIESR) is the only known technique being capable of specific HO_2 measurements in the atmosphere, but requires relatively long integration times (30 min) (Mihelcic et al., 1985, 1990).

Laser induced fluorescence (LIF) allows a more sensitive HO_2 detection, at integration times of about 1 min. It applies chemical conversion of HO_2 to OH at reduced pressure and detects OH by LIF (see review, Heard and Pilling, 2003). Chemical conversion combined with radical amplification

is used by Peroxy Radical Chemical Amplifier (PERCA) (Cantrell et al., 1984; Hastie et al., 1991; Clemitshaw et al., 1997; Burkert et al., 2001; Sadanaga et al., 2004; Mihele and Hastie, 2000; Green et al., 2006; Andrés-Hernández et al., 2010) and Peroxy Radical Chemical-Ionization Mass Spectrometry (ROxMas, PerCIMS) (Hanke et al., 2002; Edwards et al., 2003; Hornbrook et al., 2011), in order to achieve high measurement sensitivities for HO$_2$. All indirect techniques (LIF, PERCA and ROxMas/PerCIMS) make use of the conversion reaction between HO$_2$ and NO, in order to produce OH. Possible loss of OH by formation of nitrous acid (HONO) can be suppressed by lowering the pressure in the measurement systems.

$$HO_2 + NO \rightarrow OH + NO_2 \tag{R1}$$

$$OH + NO + M \rightarrow HONO + M \tag{R2}$$
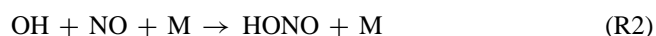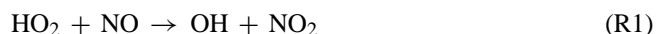
M is any collision partner, mostly oxygen and nitrogen.

Organic peroxy radicals (RO$_2$) are present in the atmosphere at similar concentrations as HO$_2$. RO$_2$ is mainly produced in the reactions of OH, O$_3$ and NO$_3$ with organic compounds. Reactions of VOCs with OH take place either via H-atom abstraction or addition of OH leading to two different types of RO$_2$ radicals (Atkinson and Arey, 2003). RO$_2$ radicals react with NO at nearly the same rate as HO$_2$.

$$RO_2 + NO \rightarrow RO + NO_2 \tag{R3}$$

$$RO + O_2 \rightarrow R'CHO + HO_2 \tag{R4}$$

$$RO + NO \rightarrow RONO \tag{R5}$$
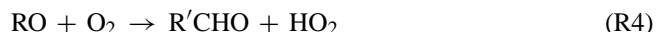
In HO$_2$ detection systems that apply chemical conversion HO$_2$ produced by Reaction (R4) can undergo further conversion to OH (Reaction R1). This is utilized by PERCA and ROxMas/PerCIMS instruments, and one specialized LIF instrument, ROxLIF (Fuchs et al., 2008), in order to measure the sum of HO$_2$ and RO$_2$ (= RO$_x$). PERCA instruments cannot distinguish between HO$_2$ and RO$_2$. ROxMas/PerCIMS instruments, however, modulate the chemical conditions in their instruments, in order to measure either RO$_x$, or HO$_2$ only. The HO$_2$ measurement mode requires good suppression of the RO$_2$ to HO$_2$ conversion. Edwards et al. (2003), for example, achieved a suppression to less than 15 % in their PerCIMS instrument for RO$_2$ species that were produced by the reaction of Cl with various hydrocarbons. However, this required large changes in concentrations of reactants, so that the modulation between HO$_2$ and RO$_x$ measurement mode took 30 min. In order to achieve a faster switching of the measurement modes within 1 min, Hornbrook et al. (2011) lowered the reactant concentrations in the HO$_2$-mode. The new method that improves temporal resolution offers good discrimination between HO$_2$ and various alkyl peroxy radicals, but RO$_2$ from the reaction of OH with large alkanes, alkenes (including isoprene) and aromatics are partially or

fully detected in the HO$_2$-mode of this instrument. RO$_2$ radicals were produced by the reaction of OH in Hornbrook et al. (2011), so that radical species from the same organic precursor were not necessarily the same as in Edwards et al. (2003).

It is generally believed that RO$_2$ radical conversion via Reactions (R3), (R4) and (R1) in the detection cell of LIF instruments for HO$_2$ measurements is negligible (Heard and Pilling, 2003). Experimental investigations in the laboratory for C$_1$–C$_4$ alkyl peroxy radicals and results from field campaigns (Stevens et al., 1994; Mather et al., 1997; Kanaya et al., 2001; Creasey et al., 2002; Ren et al., 2004; Fuchs et al., 2010) did not hint towards a significant interference. For example, for the instrument characterized here, it was shown that the upper limit for an interference from methyl peroxy radicals (CH$_3$O$_2$) is 5 % (Weber, 1998; Holland et al., 2003). The reason for the suppression of OH formation from CH$_3$O$_2$ radicals is the slow rate of Reaction (R4) at the low-pressure condition in the instrument. Only a small fraction of CH$_3$O is eventually converted to OH within the reaction time of a few milliseconds between the injection of NO and detection by the laser beam. Moreover, Reaction (R4) competes with the formation of nitrite in the presence of high NO concentrations (Reaction R5). However, the potential for an interference from organic peroxy radicals from alkenes, aromatics and OVOCs was not experimentally studied assuming that these RO$_2$ radicals would behave like small alkyl peroxy radicals.

So far, only few intercomparisons of HO$_2$ concentration measurements from different instruments have been performed at atmospheric conditions. The HO$_2$ comparisons in ambient air between LIF and MIESR (Platt et al., 2002) and between LIF and PerCIMS (Ren et al., 2003) exhibited high correlations and good absolute agreement without hints towards significant interferences. Recently, however, Ren et al. (2008) reported a change of the calibration factor of the LIF instrument. This may possibly require revision of the comparison results. Good agreement was also found for measurements from ROxLIF and MIESR in chamber measurements, during which HO$_2$, CH$_3$O$_2$ and C$_2$H$_5$O$_2$ were specifically measured (Fuchs et al., 2009). However, unexplained differences were observed between three LIF instruments in the international comparison campaign HOx-Comp (Fuchs et al., 2010), when measurements were taken in ambient air and in chamber experiments. Although the data from different instruments were well-correlated, the linear regressions showed sometimes differences that exceeded the combined estimated measurement errors and exhibited an unexplained water vapor dependence. The results from this campaign point to potential interferences in the calibration or measurement techniques.

Therefore, we investigated (1) the yield of radicals in the calibration source that produces OH and HO$_2$ radicals by water photolysis at 185 nm and (2) the potential for an interference from various RO$_2$ radical species in HO$_2$ concentration measurements. RO$_2$ radicals are produced by the reaction of
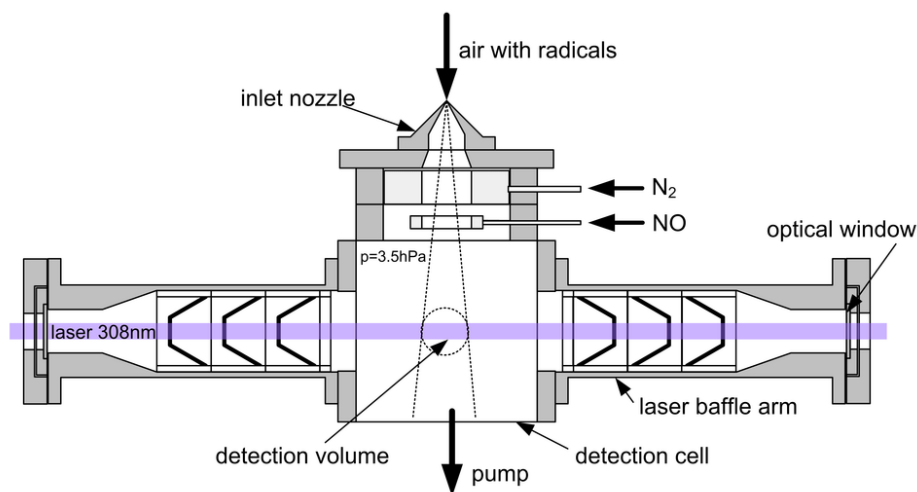
Fig. 1. Schematic drawing of the experimental setup. Peroxy radicals are converted to OH in their reaction with NO, which is injected into the gas expansion downstream of the inlet nozzle, in the low pressure detection cell. The air is exposed to pulsed laser radiation at 308 nm and the resulting fluorescence from OH is detected in the direction perpendicular to the laser and gas beam. For experiments done here, air is sampled from a calibration source, which provides either OH and HO_2, exclusive HO_2 or HO_2 and RO_2 radicals.

organic compounds with OH in the calibration source. An interference from RO_2 radicals would impact HO_2 concentration measurements in the past, when high loads of VOCs including isoprene were present such as during the field campaigns ECHO (Kleffmann et al., 2005; Dlugi et al., 2010) and PRIDE-PRD2006 (Hofzumahaus et al., 2009; Lu et al., 2011).

2 Detection of HO₂ radicals

HO_2 radicals cannot be detected directly by LIF. However, they can be chemically converted to OH, so that the detected OH concentration represents the sum of HO_2 and OH ($= HO_x$) in the sampled air (Hard et al., 1984; Heard and Pilling, 2003). A description of our LIF instrument has been given by Holland et al. (2003). The main instrument parameters are summarized in Table 1 and a schematic drawing of the detection cell is given in Fig. 1. The instrument performed measurements in two configurations: In the first configuration, 0.28 slpm (liter per minute at 1 atm and 20 °C) of air is drawn into a detection cell at low pressure of 3.5 hPa through a conically shaped inlet nozzle (Beam Dynamics) with an orifice of 0.2 mm. Configuration 2 differs in the orifice size of the inlet nozzle (0.4 mm), so that 1.1 slpm is drawn into the detection cell. The latter instrument configuration was used in past field campaigns and for experiments in the simulation chamber SAPHIR in Jülich.

The air stream in the detection cell is crossed by a short laser pulse at 308 nm (25 ns duration, 8 mm diameter, 8.5 kHz repetition rate, 25 mW average power at 308 nm), which is provided by a Nd:YAG pumped dye laser system (Navigator Spectraphysics and Intradye Laser Analytical

Table 1. Properties of the instrument regarding the HO_2 detection.

	Config. 1	Config. 2[a]
Inlet orifice/mm	0.2	0.4
Sample flow rate/slpm	0.28	1.1
[NO]/10^{12} cm⁻³	1–40	5–100
Distance nozzle − detection/cm	10	
Distance NO addition − detection/cm	5.5	
Conversion reaction time/ms	0.18[b]	2.7[b]
Cell pressure/hPa	3.5	
Laser rep. rate/kHz	8.5	
Laser power/mW	35–40	
Laser beam diameter/mm	8	
1 σ accuracy of the calibration/%	±10	

[a] Configuration during previous field campaigns. [b] Determined from experiments here.

Systems), approximately 10 cm downstream of the tip of the inlet nozzle (Fig. 1). OH is excited on a single rovibronic transition ($Q_{11}(3)$ line) of the $A^2\Sigma - X^2\Pi(0,0)$ transition). The resonance fluorescence is measured by gated photon counting using a time delay, in order to discriminate the OH fluorescence from the instantaneous laser stray light.

Chemical conversion of HO_2 to OH is accomplished by its reaction with NO (Reaction R1). Different flows of NO were injected into the sampled gas. During the ECHO and HOx-Comp campaigns, 4 sccm (1 sccm = 1 cm³ min⁻¹ at 298 K and 1 atm) of pure NO were added through a ring made of glass tubing with small holes, surrounding the gas expansion. During the PRIDE-PRD2006 campaign, 1 sccm of NO was injected by a glass tube with a small orifice that reached into the gas expansion. The concentration of NO was chosen that

the HO$_2$ conversion efficiency is larger than 90 % within the travel time of the sampled gas between NO addition and laser excitation (distance here: 5.5 cm). No significant difference was found in this work between using the glass ring or glass tube for NO addition. The NO was always purified in a cartridge that was filled with Ascarite (sodium hydroxide-coated silica) prior to addition. Ascarite removes gaseous nitrous acid (HONO), which can be photolyzed to OH by the 308 nm laser radiation and leads to an artificial laser-generated OH signal. With purification of NO the interference can be neglected.

3 Calibration of the detection sensitivity

3.1 The radical source

In order to calibrate the sensitivity of the LIF instrument, a radical source provides accurately known radical concentrations. This is accomplished by the photolysis of water in air at 1 atm using 185 nm radiation of a low-pressure discharge mercury lamp (Aschmutat et al., 1994; Schultz et al., 1995; Heard and Pilling, 2003):

$$H_2O + h\nu \rightarrow OH + H \quad (\lambda = 184.9 \text{ nm}) \quad \text{(R6)}$$
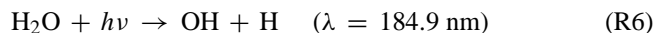
Characterization measurements reported here are done with the calibration source described in detail by Holland et al. (2003). Typical radical concentrations are 7×10^9 cm^{-3}, but can be lowered by a factor of 100 by reducing the intensity of the radiation, when the light passes an absorption cuvette filled with N$_2$O (not done here). Humidified synthetic air of highest purity (99.9999 %) flows through a 60 cm long glass tube (inner diameter 1.9 cm) at a high flow rate of 20 L min^{-1} (laminar flow). The radiation of a mercury lamp crosses the air approximately 6 cm upstream of the inlet nozzle of the instrument, which sticks into the glass tube. The transport time of the radicals produced by photolysis (Reaction R6) is approximately 20 ms, before the gas flow reaches the tip of the inlet nozzle. Radical loss inside the radical source does not play a role, since only a small part of the entire flow is sampled from the center of laminar flow. The absolute radical concentration provided by the calibration source can be related to the amount of ozone that is simultaneously formed by the photolysis of oxygen at 185 nm in the air flow (Aschmutat et al., 1994; Schultz et al., 1995):

$$O_2 + h\nu \rightarrow O + O \quad \text{(R7)}$$

$$O + O_2 + M \rightarrow O_3 + M \quad \text{(R8)}$$

Here, this is accomplished indirectly by observing the light intensity measured by a CS-I-phototube, which was calibrated against ozone production. Spectral characteristics of the phototube and an interference filter (185 nm, FWHM = 27.5 nm) in front of the phototube ensure that only radiat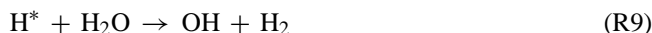ion which is relevant for the photolysis is detected by the phototube. The concentration of OH radicals produced by the calibration source can be calculated as:

$$[\text{OH}]_0 = [\text{O}_3] \frac{\Phi_{\text{OH}} [\text{H}_2\text{O}] \sigma_{\text{H}_2\text{O}}}{\Phi_{\text{O}_3} [\text{O}_2] \sigma_{\text{O}_2}} \quad (1)$$

Φ_{OH} and Φ_{O_3} are the quantum yields for OH and O$_3$. The absorption spectrum of oxygen is highly structured in the Schumann-Runge bands around 185 nm. Therefore, the value of the absorption cross section, σ_{O_2}, is specific for every mercury lamp and depends on the special design of the radical source (Hofzumahaus et al., 1996; Cantrell et al., 1997; Creasey et al., 2000). The absorption cross section of water, $\sigma_{\text{H}_2\text{O}}$, does not show distinctive structures and is well-known (Hofzumahaus et al., 1996; Cantrell et al., 1997; Creasey et al., 2003). The quantum yield of ozone in 1 atm of air is assumed to be $\Phi_{\text{O}_3} = 2$, supported by the experimental study by Washida et al. (1971). For OH, the quantum yield is generally assumed to be one based on spectroscopic considerations.

3.2 OH and HO$_2$ yields in the radical source

Photolysis of water molecules at 185 nm has only one energetically and spin-allowed dissociation channel, leading to OH($^2\Pi$) + H(^2S) with both fragments in their electronic ground states (Reaction R6). The photo-dissociation process occurs in the first absorption band of water and is experimentally and theoretically one of the best understood polyatomic photo-dissociation processes (Engel et al., 1992). Upon photon absorption, the excited H$_2$O molecule decomposes rapidly in less than an internal vibrational period. Unity quantum yield is therefore expected for OH from Reaction (R6). OH radicals are produced almost exclusively in their vibrational ground state and most of the excess energy ($\approx$1.58 eV) from the photo-dissociation is transferred into translation of the H-atoms. The highly energetic H-atoms can undergo several chemical reactions or loose their energy by collisions with other molecules:

$$H^* + H_2O \rightarrow OH + H_2 \quad \text{(R9)}$$

$$H^* + O_2 \rightarrow OH + O \quad \text{(R10)}$$

$$H^* + M \rightarrow H + M \quad \text{(R11)}$$

$$H + O_2 + M \rightarrow HO_2 + M \quad \text{(R12)}$$

Because Reaction (R11) quickly removes excess energy, it is generally assumed that the H-atoms from water photolysis are completely converted to HO$_2$ (Reaction R12). However, Reactions (R9) and (R10) are energetically possible, if the H-atoms carry translational energy greater than 0.7 eV (Bajeh et al., 2001; Zhang et al., 2000), which is the case at 185 nm. In order to investigate the relevance of OH formation from Reactions (R9) and (R10), the HO$_x$ partitioning in the calibration gas is measured, when humidified synthetic

air is irradiated by 185 nm at 1 atm, room temperature and 30 % relative humidity. The experiment is performed in two steps. First, an amount of 60 ppmv CO is added as an OH scavenger, in order to convert all OH to HO$_2$ within the residence time ($\approx$20 ms) between photolytical generation and intake into the detection cell.

$$OH + CO + O_2 \rightarrow HO_2 + CO_2 \qquad (R13)$$
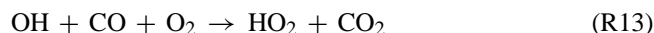
In this mode, the sum of OH and HO$_2$ is measured. OH that is produced by water photolysis (Reaction R6) and Reactions (R9) and (R10) is converted to HO$_2$ and is measured in the detection cell together with HO$_2$ produced by Reactions (R11) and (R12). Overall, this calibration mode has an HO$_2$ yield of 2 independent of Reactions (R9) and (R10). Second, 0.1 % deuterated methane (CD$_4$) is used as an scavenger, which ultimately removes OH in the calibration gas.

$$OH + CD_4 + O_2 \rightarrow CD_3O_2 + HDO \qquad (R14)$$
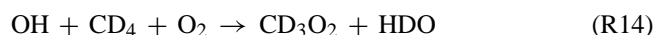
In this mode, HO$_2$ is formed by Reactions (R11) and (R12), only. If the competing Reactions (R9) and (R10) play a role, H atoms are converted to OH and the yield of HO$_2$ from Reaction (R12) is diminished, accordingly. Products of the OH-scavenging Reaction (R14) will not interfere, because the deuterated CD$_3$O$_2$ radicals cannot be converted to hydrogen-containing HO$_x$ radicals, which would be detectable at the probing laser wavelength. Overall, the calibration mode with CD$_4$ has an expected HO$_2$ yield of one, if Reactions (R9) and (R10) are negligible, or less less than one, if H-atoms are removed by Reactions (R9) or (R10).

Figure 2 shows an example of signals from one experiment, when either CO or CD$_4$ is added to the humidified air in the calibration source. The ratio of the signals gives the ratio of HO$_2$ to HO$_x$ radicals produced in the radical source. The experiment was repeated four times on different days. The mean of the ratio is 0.50 $\pm$ 0.02, meaning a ratio of quantum yields for OH and HO$_2$ of one in the photolysis of water in air. This result proves that the assumption of equal OH and HO$_2$ production in the photolysis of water at 185 nm is justified.

3.3 HO$_2$ and RO$_2$ yields of the radical source

The radical source can be operated to provide only HO$_2$ radicals by adding 60 ppmv CO to the synthetic air, in order to convert OH to HO$_2$ quantitatively (Reaction R13). This way the source provides HO$_2$ radicals with a quantum yield of two (HO$_2$-mode) in contrast to a yield of one without the addition of an OH scavenger (HO$_x$-mode). Therefore, the HO$_2$ concentration in the HO$_2$-mode is twice as large as the OH concentration defined in Eq. (1).

In a similar way, specific RO$_2$ radicals can be generated by scavenging all OH radicals with a hydrocarbon (Fuchs et al., 2008; Qi et al., 2006; Hornbrook et al., 2011). This is called the RO$_x$-mode mode of the calibration source. Again, the
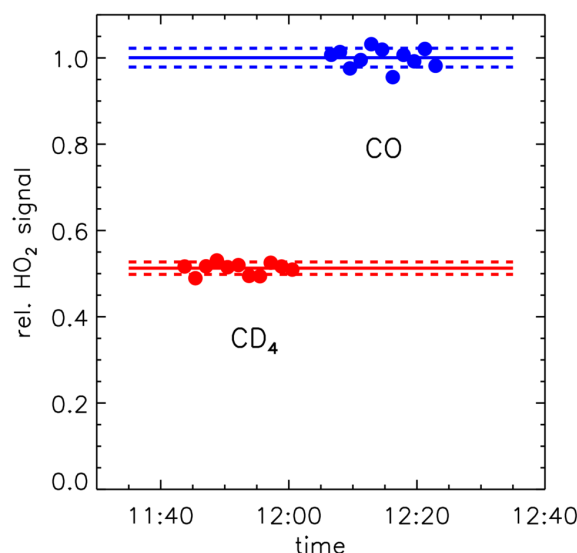

Fig. 2. Relative HO$_2$ signals if either CO or CD$_4$ is used as an OH scavenger in the calibration source. Symbols show individual measurement points, solid lines denote average values and dashed lines represent 1 σ standard deviations of measurements.

concentration of organic compounds is chosen, so that all OH is consumed within the time between production of OH in the radical source and sampling by the instrument (OH reactivity approximately 300 s^{-1}). Since hydrocarbons were added upstream of the photolysis region of the radical source, photolysis of these hydrocarbons at 185 nm may occur (Demers et al., 1978; Giroux et al., 1989). In order to test for effects of photolysis on experiments conducted here, the fluorescence signal was measured, when hydrocarbons were mixed in dry air, so that radicals are only produced by photolysis of the hydrocarbon. No significant radical production from hydrocarbon photolysis could be detected by LIF.

Different types of reactions can occur: (1) RO$_2$ radicals can be produced via H abstraction in the case of alkanes leading to alkyl peroxy radicals. (2) For other organic compounds like alkenes OH addition leads to the formation of β-hydroxyalkyl peroxy radicals (Atkinson and Arey, 2003). If RO$_2$ radicals are the only radical product, the source yields equal concentrations of RO$_2$ and HO$_2$. However, the yield of RO$_2$ radicals can differ from unity, if other product channels compete with RO$_2$ formation in the reaction of OH and the hydrocarbon. For example, it is known that part of the products of benzene with OH is HO$_2$ (prompt HO$_2$) and only 35 % is RO$_2$ (Nehr et al., 2011).

3.4 Calibration of detection sensitivities

For calibration of OH, HO$_2$ and RO$_2$ sensitivities, C_i, the radical source is operated either in the HO$_x$-, HO$_2$- or RO$_x$-mode. Sensitivities defined here and throughout this report always refer to sensitivities of the HO$_2$-cell, when NO is

added into the detection cell. The fluorescence signal measured by the LIF instrument in the three operational modes of the radical source are:

$$S_{HO_x} = C_{HO_2} \phi_{HO_2} [OH]_0 + C_{OH} \phi_{OH} [OH]_0 \qquad (2)$$

$$= (C_{HO_2} + C_{OH}) [OH]_0$$

$$S_{HO_2} = C_{HO_2} \phi'_{HO_2} [OH]_0 = 2 C_{HO_2} [OH]_0 \qquad (3)$$

$$S_{RO_x} = C_{HO_2} \phi''_{HO_2} [OH]_0 + C_{RO_2} \phi_{RO_2} [OH]_0 \qquad (4)$$

$$= (C_{HO_2} (1 + \delta) + C_{RO_2} (1 - \delta)) [OH]_0$$

ϕ_{HO_2}, ϕ'_{HO_2} and ϕ''_{HO_2} are the HO$_2$ yields in the three modes of the radical source and ϕ_{OH} and ϕ_{RO_2} the yields of OH and RO$_2$ in the HO$_x$- and RO$_x$-mode, respectively, as discussed in the previous section. The concentration [OH]$_0$ is calculated from Eq. (1). δ is the yield of prompt HO$_2$ in the reaction of organic compounds with OH without the formation of RO$_2$ on the time scale of the transport time in the radical source (20 ms).

In order to calculate the HO$_2$ detection sensitivity, only one measurement with the radical source in the HO$_2$-mode is required. In contrast, the OH sensitivity of the HO$_2$ detection cell can be calculated from the difference between measurements with the radical source in the HO$_2$- and HO$_x$-mode and the RO$_2$ sensitivity from the difference between measurements in the HO$_2$- and RO$_x$-mode:

$$C_{OH} = \frac{2 S_{HO_x} - S_{HO_2}}{2 [OH]_0} \qquad (5)$$

$$C_{HO_2} = \frac{S_{HO_2}}{2 [OH]_0} \qquad (6)$$

$$C_{RO_2} = \frac{2 S_{RO_x} - S_{HO_2} (1 + \delta)}{2 [OH]_0 (1 - \delta)} \qquad (7)$$

In a simple model, the sensitivities C_i can be expressed as a product of three generic parameters:

$$C_i = \gamma_i \, \epsilon_i \, \beta_{OH} \quad \text{with} \quad i = OH, HO_2, RO_2 \qquad (8)$$

γ_i represents the fraction of radical species i that are transmitted through the instrument inlet. ϵ_i denotes the yield of OH after the sampled radical species i has passed the distance from the gas inlet (nozzle) to the detection volume, and β_{OH} is the internal detection efficiency of OH in the detection volume. Among these parameters, ϵ_i and β_{OH} are influenced by the injected NO. More specifically, ϵ_i accounts for NO-dependent Reactions (R1) to (R5), which determine the fraction of OH that reaches the detection volume. ϵ_i represents the loss of OH by HONO formation for sampled OH (Reaction R2), while it represents the efficiency of chemical conversion to OH for sampled peroxy radicals. In principle, β_{OH} is influenced by NO-dependent quenching of the OH fluorescence, but this effect is small for the NO concentrations used in this work.

4   Experimental results for detection sensitivities

4.1   OH and HO$_2$ detection sensitivities

In order to investigate the HO$_2$ and OH detection sensitivities, the instrument sampled from the calibration source in the HO$_2$- and HO$_x$-mode of the radical source. We define the relative HO$_2$ detection sensitivity of the instrument, α_{HO_2}, as the ratio of the calibration factors for HO$_2$ and OH (Eq. 8) that can be calculated from measurements using Eqs. (5) and (6). This gives the HO$_2$ conversion efficiency weighted by the ratio of the inlet transmission efficiencies for HO$_2$ and OH:

$$\alpha_{HO_2} = \frac{C_{HO_2}}{C_{OH}} = \frac{\gamma_{HO_2}}{\gamma_{OH}} \frac{\epsilon_{HO_2}}{\epsilon_{OH}} \qquad (9)$$

Furthermore, we determine the influence of NO on the OH detection sensitivity as:

$$\epsilon_{OH} = \frac{C_{OH} (NO)}{C_{OH} (NO = 0)} \qquad (10)$$

Figure 3 shows α_{HO_2} (upper panel) and ϵ_{OH} (lower panel) depending on the NO concentration for the two different inlet nozzles (reaction times) tested here. For high NO concentrations relative detection sensitivities are approximately constant at a value larger than one. The dashed vertical line in Fig. 3 indicates the NO concentration, at which the LIF instrument (with the 0.4 mm nozzle) was operated during field campaigns in the past. Measurements show that the HO$_2$ conversion in the detection is nearly complete for this NO concentration.

The OH sensitivity, which is shown in the lower panel of Fig. 3, is nearly independent of the NO concentration within the range tested here and decreases only slightly for large NO concentrations.

4.2   RO$_2$ detection sensitivities

The potential for an OH signal caused by the conversion of RO$_2$ to HO$_2$ via Reactions (R3) and (R4) and subsequent conversion to OH is investigated for various RO$_2$ radicals. Like for HO$_2$ we define the relative RO$_2$ detection sensitivity as the ratio of calibration factors for RO$_2$ and HO$_2$ (Eq. 8), which can be calculated from measurements using Eqs. (7) and (6):

$$\alpha_{RO_2} = \frac{C_{RO_2}}{C_{HO_2}} = \frac{\gamma_{RO_2}}{\gamma_{HO_2}} \frac{\epsilon_{RO_2}}{\epsilon_{HO_2}} \qquad (11)$$

The experimental determination of the relative RO$_2$ detection sensitivity is only possible, if the yield of prompt HO$_2$ is known (δ in Eq. 7). α_{RO_2} represents the value of the interference from RO$_2$ radicals. It always refers to the HO$_2$ detection sensitivity of the instrument that is achieved for the same operational conditions.
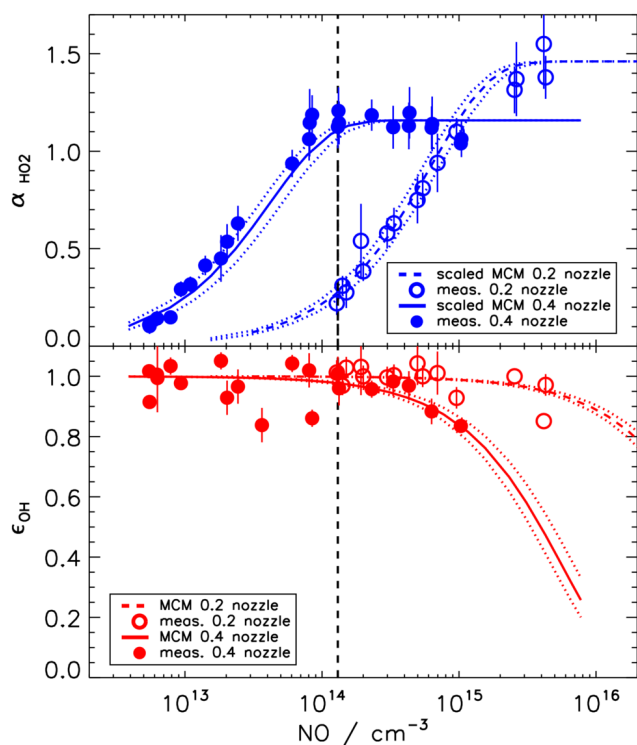
Fig. 3. Relative OH sensitivity (lower panel) and HO$_2$ (upper panel) conversion efficiency to OH depending on the NO concentration in the detection cell. Measurements (symbols) are compared to calculations using MCMv3.1 (lines). Two inlet nozzles with different orifices (0.2 and 0.4 mm) were used, in order to vary the reaction time for the conversion in the cell (0.18 and 2.7 ms). Dotted lines give results from sensitivity runs of the model varying the reaction time by ±0.025 and ±0.5 ms, respectively. The vertical dashed line indicates the working point for the instrument with the 0.4 mm nozzle in the past.

In this work, values for the relative detection sensitivity for various peroxy radicals were determined. Results are summarized in Table 2 and examples of the measurements are shown in Fig. 4 for methane, Fig. 5 for isoprene and Fig. 6 for benzene.

Alkyl peroxy radicals are produced by the reaction of an alkane with OH in the radical source. Initial H-atom abstraction is followed by the reaction of the alkyl radical with O$_2$ (Atkinson and Arey, 2003) producing alkyl peroxy radicals. The relative detection sensitivity for methyl peroxy radicals, which are produced in the reaction of methane with OH, is below the limit of detection of the instrument for the configuration of the instrument with the 0.2 mm nozzle for the range of NO concentration tested here (open circles in Fig. 4). For the larger orifice, however, a small interference of 0.04 ± 0.04 is measured for the NO concentration, at which the cell was operated in the field (filled circle at dashed vertical line). Measurements exhibit a maximum of nearly 0.1 at smaller NO concentrations. This behavior was reproduced in several experiments.
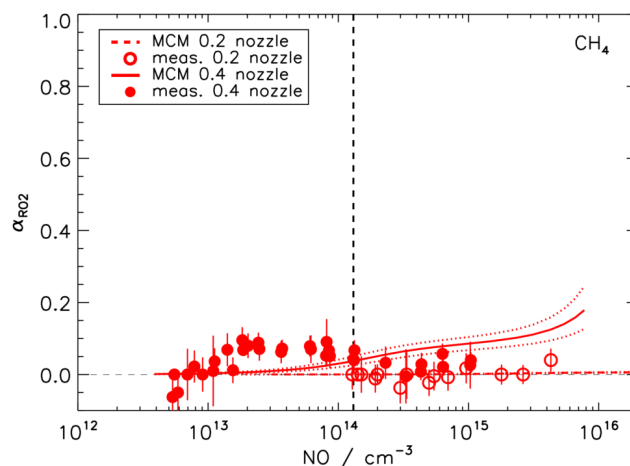

Fig. 4. Relative detection sensitivity for RO$_2$ radicals produced by methane and OH depending on the NO concentration in the detection cell. Measurements (symbols) are compared to calculations using MCMv3.1 (solid line) with non-zero initial RO$_2$ and zero HO$_2$ concentration. Two inlet nozzles with different orifices (0.2 and 0.4 mm) were used, in order to vary the reaction time for the conversion in the cell. Reaction times determined from the HO$_2$ conversion efficiency were used for model calculations and were varied according to the uncertainty of the reaction time, ±0.025 and ±0.5 ms (dotted lines). The vertical dashed line indicates the working point for the instrument with 0.4 mm nozzle in the past.
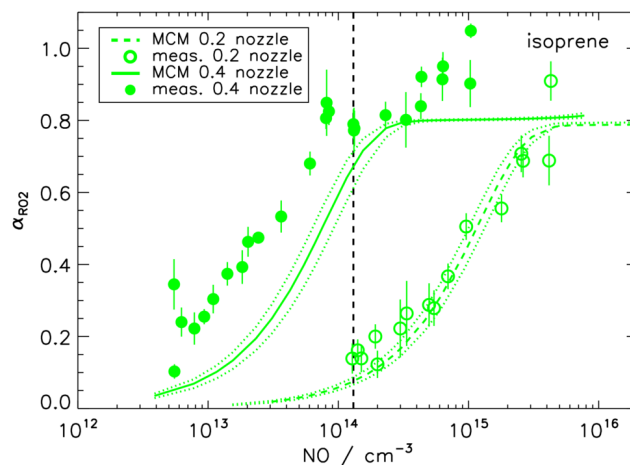

Fig. 5. Same as Fig. 4, but for RO$_2$ radicals produced by isoprene and OH.

Relative detection sensitivities are investigated for two other alkyl peroxy radicals, ethyl peroxy and cyclohexyl peroxy radicals, from the reaction of OH with ethane and cyclohexane, respectively, for two configurations of the detection cell (Table 2). For the configuration using the 0.4 mm orifice, the relative detection sensitivity of 0.07 ± 0.03 is small for ethyl peroxy radicals, but it is significantly larger for cyclohexyl peroxy radicals (0.48 ± 0.14). It is reduced to values

Table 2. Measured and calculated relative detection sensitivities of different RO$_2$ species in the HO$_2$ detection cell for two inlet configurations. Modeled values are calculated from the ratio of conversion efficiencies that are achieved for RO$_2$ and HO$_2$ ($\alpha'_{RO_2} = \frac{\epsilon_{RO_2}}{\epsilon_{HO_2}}$) assuming $\gamma_{RO_2} = \gamma_{HO_2}$ (Eq. 11). The sensitivity applies for RO$_2$ that is produced in the reaction of organic precursors with OH and O$_2$.

	Orifice 0.4 mm [NO] = 1.3 × 10^{14} cm^{-3}		Orifice 0.2 mm [NO] = 1.2 × 10^{14} cm^{-3}	
Precursor	α_{RO_2} (exp.)	α'_{RO_2} (model)	α_{RO_2} (exp.)	α'_{RO_2} (model)
Methane	0.04 ± 0.04	0.04	−0.01 ± 0.02	0.00
Ethane	0.07 ± 0.03	0.18	0.01 ± 0.02	0.00
Cyclohexane	0.48 ± 0.14	10.14[a]	0.03 ± 0.00	10.00[a]
Ethene	0.85 ± 0.05	0.85	0.17 ± 0.03	0.08
Propene	0.95 ± 0.03	0.83	0.15 ± 0.03	0.08
Isoprene	0.79 ± 0.05	0.67	0.1 2 ± 0.02	0.07
MVK	0.60 ± 0.06	20.26[b]	0.24 ± 0.11	20.03[b]
MACR	0.58 ± 0.04	0.38	0.14 ± 0.02	0.00
Benzene	0.86 ± 0.11[c]	0.78	0.17 ± 0.17[c]	0.08

[a] MCMv3.1 does not include decomposition of the cyclohexoxy radical. [b] MCMv3.1 does not include all reaction paths of the RO$_2$ radical from MVK.
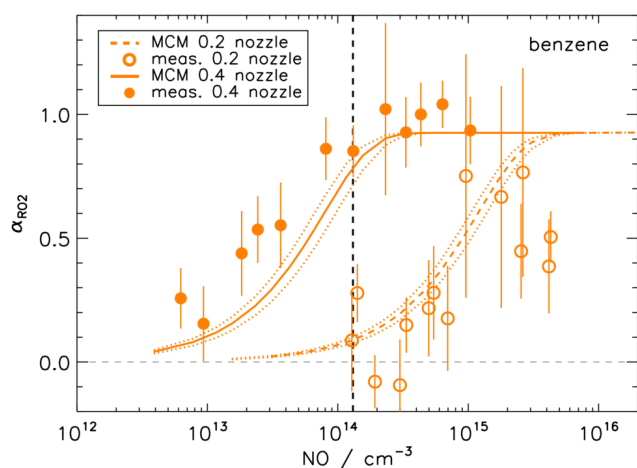[c] Value does not include 65 % prompt HO$_2$ formation in the radical source.

Fig. 6. Same as Fig. 4, but for RO$_2$ radicals produced by benzene and OH. Measurements take 65 % of prompt HO$_2$ formation in the radical source into account.

within the range of the limit of detection of the instrument for the configuration with the 0.2 mm orifice for both radical species.

The major pathway of the reaction of OH with alkenes is its addition to the carbon atoms of the double-bond forming a β-hydroxyalkyl radical, which then reacts with O$_2$ to form the corresponding β-hydroxyalkyl peroxy radical (Atkinson and Arey, 2003). Relative detection sensitivities were measured for radicals for the peroxy radicals from the OH reaction with ethene, propene and isoprene. All of them show a high relative detection sensitivity (Table 2) for the configuration with the 0.4 mm nozzle with 0.85 ± 0.05, 0.95 ± 0.03 and 0.79 ± 0.05 for radicals

from ethene, propene and isoprene, respectively. The values are significantly reduced (0.17 ± 0.03, 0.15 ± 0.03 and 0.12 ± 0.02) for the configuration with the 0.2 mm nozzle. Figure 5 shows the dependence of the relative detection sensitivity on the NO concentration in the detection cell for RO$_2$ radicals from isoprene plus OH, emphasizing the NO dependence of the relative detection sensitivity. The high relative detection sensitivities suggest a fast conversion of β-hydroxyalkoxy radicals to HO$_2$. This means that RO$_2$ radicals from isoprene produced a strong interference signal for HO$_2$ measurements by the LIF-instrument in the past.

Relative detection sensitivities for RO$_2$ radicals from MVK and MACR are shown in Table 2. They are smaller than that measured for ethene and propene for the configuration used in field campaigns (0.4 mm nozzle), but are still significant (MVK: 0.60 ± 0.06, MACR: 0.58 ± 0.04). They are reduced to values within the range of values for other alkenes (MVK: 0.24 ± 0.11, MACR: 0.14 ± 0.02), if the smaller orifice (shorter reaction time) is used.

The reaction of benzene with OH is an example for prompt formation of HO$_2$ within the transport time of the calibration gas in the radical source ($\delta > 0$ in Eq. 7). The formation of HO$_2$ in air is fast (2.2 ms) (Bohn and Zetzsch, 1999), much shorter than the travel time of air between photolysis and sampling by the instrument. A yield of 65 % recommended in literature based on product studies in the EUPHORE chamber (Bloss et al., 2005a,b) is taken for calculations using Eq. (7). We investigated recently the yield of prompt HO$_2$ formation by directly observing the HO$_2$ formation and found good agreement (Nehr et al., 2011). Here, the relative detection sensitivity for RO$_2$ radicals from benzene plus OH was found to be approximately 0.9 for high NO concentrations for the two configurations with the different inlet

nozzles (Fig. 6). It is approximately 0.85 at the working point of the 0.4 mm nozzle used in previous field campaigns. The relative detection sensitivity decreases with decreasing NO concentration and is smaller than 0.1 for the 0.2 mm nozzle at the lowest NO concentration tested here.

4.3 Water dependence of HO₂ and RO₂ detection sensitivities

The measurement intercomparison for HO₂ by different LIF instruments during HOxCOMP revealed discrepancies that were apparently correlated with the atmospheric water vapor (Fuchs et al., 2010). This result was surprising, because all instruments had corrected their measurements for the known influence of OH fluorescence quenching by water vapor. Results from this campaign must therefore be considered as a hint to a so far unknown water-related interference. For this reason, the water vapor dependence of our LIF detection sensitivity for HO₂ was reinvestigated (Fig. 7).

In the upper panels, the calibration factors for HO₂ and RO₂ are shown, both of which decrease with increasing water vapor concentration in the same way. The trend is compared to calculations that give the reduction of the sensitivity due to fluorescence quenching by water vapor using quenching constants from literature (Heard and Henderson, 2000). Calculations and measurements are in good agreement. This proves once more that the correction factor that was applied to measurements from this LIF instrument during HOxCOMP accounts for a dependence of the instrument sensitivity correctly. The relative detection sensitivity for the isoprene peroxy radicals does not show any significant trend with the water vapor mixing ratio for both inlet nozzles. This suggests that water vapor does not influence the overall RO₂ to OH conversion at the conditions in our measurement instrument.

5 Discussion of detection sensitivities

5.1 OH and HO₂ detection sensitivities of the LIF instrument

The relative detection sensitivities for HO₂ increases with NO and is approximately constant for high NO. In this case, the HO₂ conversion to OH is complete ($\frac{\epsilon_{HO_2}}{\epsilon_{OH}} \to 1$ in Eq. 9). The plateau value has a value of greater than one (Fig. 3, upper panel), which can be explained by different transmission efficiencies for HO₂ and OH (Eq. 9). The HO₂ inlet transmission efficiency is approximately 45 % larger than that for OH for the 0.2 mm nozzle and 15 % larger for the 0.4 mm nozzle. A larger inlet transmission efficiency for HO₂ than for OH is expected because of the generally smaller reactivity of HO₂ towards surfaces (Mihele and Hastie, 1998; Fuchs et al., 2008).

Measured α_{RO_2} values are compared to calculated values using the framework of the Master Chemical Mechanism
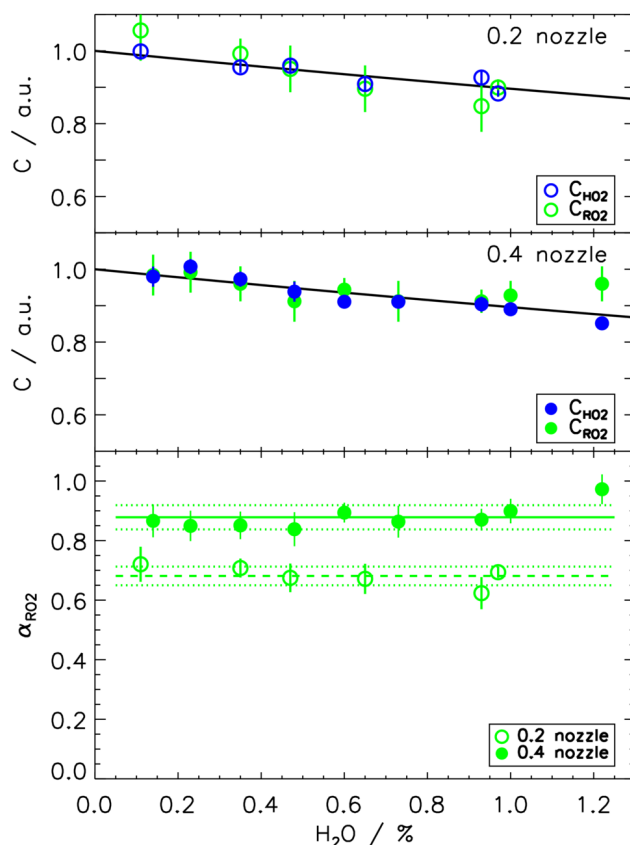

Fig. 7. Dependence of the interference from RO₂ radicals produced by isoprene and OH on water vapor (lower panel) at high NO concentrations (0.2 mm nozzle: 3×10^{15} cm⁻³, 0.4 mm nozzle: 4×10^{14} cm⁻³). Experiments were carried out for two combinations of reaction times (orifice diameters) and NO concentrations. Symbols show individual measurement points and lines are average values (solid, dashed) and 1σ standard deviations (dotted) of measurements. In the upper two panels the water vapor dependence of measured detection sensitivities for HO₂, C_{HO_2}, and RO₂ from isoprene, C_{RO_2}, (scaled to one dry conditions) is compared to calculations that give the reduction of the instrument sensitivity due to fluorescence quenching by water vapor (black lines).

version 3.1 (MCMv3.1, Saunders et al., 2003; Jenkin et al., 2003), in order to simulate the radical conversion. The initial concentration of HO₂ is set to 1×10^8 cm⁻³ for model calculations. The results of the model are independent of the initial concentration, because the much larger concentrations of the major reactants (NO, O₂) are virtually constant and radical-radical reactions play no role at the given concentrations and time scale. The ratio of the calculated OH concentration after the reaction time, which is determined as described below, and the initial HO₂ concentration gives the HO₂ conversion efficiency ϵ_{HO_2} in Eqs. (8) and (9). The ratio of inlet transmission efficiencies determined for measurements at high NO concentrations is used to scale the results of model calculations, since the model does not include inlet loss reactions.

The reaction time for radical conversion in the detection cell is determined by fitting the modeled HO$_2$ curve to the measured data in Fig. 3, upper panel. This reaction time is used as model input for all other model calculations. A reaction time of 0.18 ± 0.025 ms for the 0.2 mm nozzle and a reaction time of 2.7 ± 0.5 ms for the 0.4 mm nozzle is determined (errors are estimated from sensitivity runs). The value for the 0.2 mm nozzle is similar to previous results (Weber, 1998), but the reaction time for the 0.4 mm nozzle is much longer. Air is sampled by supersonic expansion in both cases, so that similar travel times in the detection cell may be expected.

Model calculations reproduce the NO dependence of the measured relative HO$_2$ detection sensitivities (Fig. 3). Also the NO dependence of the OH detection efficiency (Fig. 3, lower panel) is well-described. The small decrease at high NO concentrations can be explained by OH loss in its reaction with NO forming HONO (Reaction R2).

The sampled air cools down significantly when it is expanded from ambient pressure to the low pressure in the measurement instrument. Previous experiments with a nozzle orifice of 0.75 mm showed a large reduction of the rotational temperature of OH in the probing laser beam to $T = 207$ K (Holland et al., 1995). When an orifice diameter of 0.2 mm or 0.4 mm is used, the rotational temperature is found to be equal to room temperature indicating that the expanded gas has come into thermal equilibrium with the surrounding sheath gas, when it reaches the laser beam. This was also shown for another LIF instrument 40–50 mm downstream of a flat inlet nozzle with a 0.2 mm orifice (Creasey et al., 1997). In order to estimate the influence of a temperature gradient on the peroxy radical conversion along the line from the NO injection point to the detection volume, we have also performed model calculations at a reduced temperature of 230 K. The difference to model results for 295 K is small (<20 %). This is also the case for all other model calculations that are performed, in order to calculate RO$_2$ conversion efficiencies below, indicating a negligible effect of temperature on the conversion reaction schemes (as far as they are known and included in MCMv3.1).

5.2 Interference from alkyl peroxy radicals

The high NO concentration in the detection cell ensures that alkyl peroxy radicals react exclusively with NO forming alkoxy radicals (Reaction R3). The rate constant of this reaction is similar for different RO$_2$ (typically 9×10^{-12} cm^{-3} s^{-1} at 298 K) (Atkinson and Arey, 2003). In addition to alkoxy radicals alkyl nitrates can be formed, but their yield is not well-known (Atkinson and Arey, 2003). Studies show that the yield is increasing with increasing number of C-atoms in the peroxy radical and with increasing pressure (Atkinson and Arey, 2003; Zhang et al., 2004). The lifetime of peroxy radicals is approximately 1 ms for conditions, at which the detection cell was operated in the

field (0.4 mm nozzle, [NO] $= 1.3 \times 10^{14}$ cm^{-3}). Therefore, a substantial part of the alkyl peroxy radicals can be converted to alkoxy radicals within the reaction time determined from investigations of the HO$_2$ conversion efficiency (2.7 ms). Alkoxy radicals react via one or more pathways (Atkinson, 1997b; Orlando et al., 2003): (1) reaction with oxygen, (2) decomposition, (3) isomerization, (4) reaction with NO.

Model calculations (Fig. 4) that were performed to calculate the RO$_2$ conversion efficiency for methyl peroxy radicals agree with measurements for the short reaction time of the 0.2 mm nozzle showing that RO$_2$ conversion is negligible. For the longer reaction time with the 0.4 mm nozzle model calculations predict an increase of the RO$_2$ conversion efficiency with increasing NO concentrations, because of the faster conversion to HO$_2$. The small maximum in the measured RO$_2$ detection sensitivities at lower NO cannot be reproduced by model calculations using one reaction time. The reason for the discrepancy between measurements and model calculation is not clear. One may speculate that part of the sampled gas has a much longer residence time than determined from measurements of the HO$_2$ conversion efficiency due to e.g. recirculation in the background volume of the detection cell, so that a description of measurements with a single reaction time may not be sufficient. However, since CH$_3$O$_2$ is the most prominent radical for a wide range of atmospheric conditions, the important point is that there is no significant interference from methyl peroxy radicals for conditions at which the instrument was operated in the past.

The relative detection sensitivity for larger alkyl peroxy radicals may be greater than that for methyl peroxy radicals, since the reaction of alkoxy radicals, formed in the reaction of alkyl peroxy radicals with NO, with O$_2$ is faster by a factor of 4 to 6 (Atkinson and Arey, 2003; Orlando et al., 2003). Again, neither reaction rate constants nor the importance of decomposition and isomerization are well-known. Model calculations of the conversion efficiency for ethyl peroxy and cyclohexyl peroxy radicals approximately agree with measurements (Table 2). A larger discrepancy is only observed for cyclohexyl peroxy radicals, when the 0.4 mm nozzle is used. A large relative detection sensitivity of 0.48 ± 0.14 is measured, but model calculations predict only a small conversion efficiency of 0.14. This may be due to fast production of HO$_2$ from decomposition of the cyclohexoxy radical that competes with the ring maintaining reaction with O$_2$ (Aschmann et al., 1997; Orlando et al., 2000), but HO$_2$ production from this reaction has not been investigated so far. The yield of other ring-opening decomposition products was estimated to be nearly 0.50 for atmospheric conditions (Aschmann et al., 1997) similar to the relative conversion efficiency measured here. MCMv3.1 lacks any decomposition of the cyclohexoxy radical, so that it is not expected that the calculated conversion efficiency of the cyclohexyl radical agrees with measurements.

Results obtained here agree with previous investigations for our LIF instrument (Weber, 1998; Holland et al., 2003). An upper limit for an interference from methyl peroxy radicals of 0.05 was measured using the 0.2 mm nozzle. Potential interferences from small alkyl peroxy radicals in the HO₂ detection were also investigated for other LIF instruments and found to be negligible in agreement with results obtained here. Kanaya et al. (2001) investigated the detection sensitivity of an LIF instrument for ethyl peroxy radicals. A relative detection sensitivity of 0.05 was found. The potential for interferences from C_1–C_4 alkyl peroxy radicals were also experimentally investigated for another LIF instrument by Ren et al. (2004) and found to be negligible.

5.3 Interference from β-hydroxyalkyl peroxy radicals

Similar to alkyl peroxy radicals, β-hydroxyalkyl peroxy radicals can undergo conversion reactions leading finally to the formation of HO₂ in the detection cell. As an example, Fig. 8 shows the reaction sequence for β-hydroxyalkyl peroxy radical from ethene plus OH. They react with NO forming β-hydroxyalkoxy radicals with a reaction rate constant that is similar to those of alkyl peroxy radicals (Atkinson and Arey, 2003). β-hydroxyalkoxy radicals can react with O₂ or can decompose or isomerize. However, in contrast to alkoxy peroxy radicals, decomposition and isomerization appear to be the dominant pathways, except for the HOCH₂CH₂O radical (from ethene plus OH), for which decomposition and reaction with O₂ can be competitive (Atkinson, 1997a). Decomposition rate constants were determined to be on the order of 10^4 to $10^6 s^{-1}$ (Atkinson, 1997a,b; Orlando et al., 1998; Vereecken et al., 1999). Decomposition leads to the formation of a hydroxyalkyl radical, which then reacts rapidly and solely with O₂ forming a carbonyl compound plus HO₂ (Atkinson, 1997b; Orlando et al., 2003). Compared to the slow alkoxy + O₂ reaction (e.g., for CH₃O), which inhibits the overall RO₂ to OH conversion for simple alkyl peroxy radicals in our detection cell, decomposition of β-hydroxyalkoxy radicals is extremely fast. Therefore, the lifetime of the β-hydroxyalkoxy radical is much shorter than the reaction time in the detection cell for the 0.4 mm nozzle, so that they are efficiently converted to HO₂. As a consequence, the reaction with NO limits the conversion efficiency, so that a strong interference is observed for high NO concentrations that decreases with decreasing NO in contrast to assumption made in the past.

In the MCMv3.1 decomposition of the β-hydroxyalkoxy radical is lumped with the subsequent reaction of the hydroxyalkyl radical with O₂. Due to the reduced density of O₂ in the detection cell, calculations using MCMv3.1 may not accurately describe the conversion efficiency. In addition, inlet transmission efficiencies for β-hydroxyalkyl peroxy radicals may be different from that for HO₂. Despite these limitations calculated conversion efficiencies approximately match relative detection sensitivities as shown in Table 2.
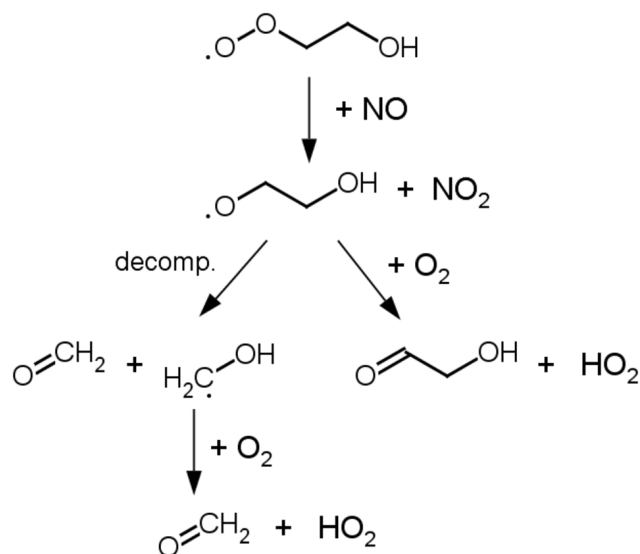

Fig. 8. Reaction scheme of the radical sequence of the β-hydroxyalkyl peroxy radical produced by the reaction of OH with ethene. The β-hydroxyalkoxy radical formed in the reaction with NO either decomposes or reacts with O₂ in contrast to other β-hydroxyalkoxy species which exclusively decompose.

5.4 Interference from RO₂ produced by isoprene + OH and its oxidation products + OH

The fate of peroxy radicals from isoprene and OH is subject of recent theoretical and experimental investigations (Peeters et al., 2009; da Silva et al., 2010). If NO is present, the reaction pathway is similar to that of an alkene, but four different hydroxyalkyl peroxy radicals can be formed (Fan and Zhang, 2004; Ghosh et al., 2010; Greenwald et al., 2010), two of which are favored (yield: 0.97). They can be converted to HO₂ in a radical reaction sequence. Peeters et al. (2009) suggest that the hydroxyalkyl peroxy radical may also undergo a 1,6-H-shift with subsequent decomposition and formation of HO₂ instead of reaction with NO. This prompt HO₂ formation may be of importance under low NO conditions. Another theoretical study by da Silva et al. (2010) suggests a high yield of HO₂ from unimolecular decomposition of the hydroxyalkyl peroxy radical to HO₂ in the absence of NO. No NO is present in the radical source, so that these reaction pathways would change the ratio of RO₂ to HO₂ towards HO₂ (Eq. 7 with $\delta > 0$).

Lines in Fig. 5 show relative conversion efficiencies of RO₂ radicals from isoprene to HO₂ from model calculations using MCMv3.1, which does not include the recently suggested prompt HO₂ formation from the hydroxyalkyl peroxy radical. Conversion efficiencies of the four peroxy radicals that are formed in the reaction of isoprene with OH are weighted averages with weights accounting for the formation yields of the peroxy radical species assumed in MCMv3.1. Although the reaction mechanism neglects details of the

conversion of the hydroxyalkoxy radicals to HO$_2$, calculations reproduce roughly the observations. The agreement is better for the 0.2 mm nozzle, whereas measurements seem to be shifted towards smaller NO concentrations for the 0.4 mm nozzle. However, one has to keep in mind that calculated conversion efficiencies need to be weighted by the ratio of the inlet transmission efficiencies for RO$_2$ and HO$_2$ to be compared to measured relative detection sensitivities (Eq. 11). They are approximately 10 % larger for the 0.4 mm nozzle at high NO concentrations than calculated conversion efficiencies. This indicates that inlet transmission efficiency for peroxy radicals from isoprene may be slightly larger than that for HO$_2$ for this nozzle. Moreover, results for methyl peroxy radicals indicates (see above) that the description of the RO$_2$ conversion with one reaction time may not be sufficient.

Measured relative detection sensitivities are larger than calculated conversion efficiencies at low NO concentrations for both inlet nozzles. The difference of 0.08 can be regarded as an upper limit for potential prompt HO$_2$ formation (Eq. 11) in the radical source as suggested by Peeters et al. (2009) and da Silva et al. (2010) within the time between formation and detection of RO$_2$ radicals (20 ms). This upper limit would be consistent with the limit of the rate constant for the 1,6-H-shift given by Peeters et al. (2009), which converts to a lifetime of 120 ms, but does not fit to results obtained by Nehr et al. (2011), who investigated prompt HO$_2$ formation on a time scale of one second. However, the same authors lowered recently the estimate for the rate constant to $0.1 \, \text{s}^{-1}$ (Peeters and Muller, 2010). In this case, the 1,6-H-shift would be too slow to be observed in experiments conducted here. The decomposition rate given by da Silva et al. (2010) for direct decomposition of the hydroxyalkyl peroxy radical (lifetime of several minutes) is too small to play a role in these experiments.

The two major atmospheric oxidation products from the degradation of isoprene with OH are MVK and MACR, both of which can be further oxidized by OH. The fate of RO$_2$ radicals from MVK and MACR plus OH are not well-known. Like for alkenes OH can add to the C = C double bond at two positions for MVK, so that two hydroxyalkyl peroxy radical species are formed. Both react with NO forming hydroxyalkoxy radicals, which further decompose. The hydroxyalkoxy radical that is formed, if OH adds at the terminal CH$_2$ group of MVK (yield: 0.64), decomposes via two channels (Tuazon and Atkinson, 1989), so that three conversion paths are possible. Two of them are similar to the reaction chain that follows the path described above for alkenes, so that a fast conversion to HO$_2$ is possible. However, decomposition products of the third channel do not lead to a fast HO$_2$ production. For this reaction path Tuazon and Atkinson (1989) measured a yield of 0.64 (referred to the entire reaction of MVK from product studies). Consequently, only the remaining part (36 %) can lead to a fast conversion of RO$_2$ to HO$_2$ in the detection cell via the other two reaction channels. The relative detection sensitivity for RO$_2$ radicals

is significantly larger (0.60) inconsistent with this reaction scheme. Calculations using MCMv3.1 (Table 2) give even smaller conversion efficiencies, since the mechanism does not include all of the conversion paths that lead to fast formation of HO$_2$.

In contrast to MVK, OH can add to MACR (yield: 0.43) or can abstract an H-atom (yield: 0.57) (Tuazon and Atkinson, 1990; Orlando et al., 1999). H-abstraction leads to the formation of an acyl peroxy radical that reacts with NO to the 1-methylvinyl radical and cannot be converted to HO$_2$ within the reaction time in the HO$_2$ detection cell. The hydroxyalkyl peroxy radical that is formed, if OH adds to MACR, follows the reaction path of other hydroxyalkyl peroxy radicals, so that HO$_2$ is formed quickly. Therefore, it is reasonable that the relative detection sensitivity for peroxy radicals (0.58 ± 0.04, Table 2) from the reaction of MACR with OH for the configuration with the 0.4 mm nozzle is within the range of the yield of hydroxyalkyl peroxy radicals (0.43) (Tuazon and Atkinson, 1990; Orlando et al., 1999). Also calculations of the conversion efficiency using MCMv3.1 (Table 2) give a relative RO$_2$ conversion efficiency that is similar to the yield of hydroxyalkyl peroxy radicals for this configuration.

5.5 Interference from RO$_2$ produced by benzene + OH

Measured detection sensitivities for RO$_2$ from benzene plus OH agrees approximately with calculated conversion efficiencies using MCMv3.1. Equations (7) and (11) with $\delta = 0.65$ are used to determine the relative detection sensitivity, so that prompt HO$_2$ formation in the radical source does not add to the relative detection sensitivity of the peroxy radical. Error bars of data are relatively large (Fig. 6), because of the small RO$_2$ concentration compared to HO$_2$ from prompt HO$_2$ formation in the radical source.

OH adds to benzene forming the hydroxycyclohexadienyl radical, which reacts predominantly with O$_2$ in air (Nehr et al., 2011). Products are phenol plus HO$_2$ (yield: 0.53, Volkamer et al., 2002) and RO$_2$ radicals, part of which most likely decomposes to epoxides and HO$_2$ (yield: 0.12, Bloss et al., 2005b). Only 0.35 of the products in the reaction of benzene with OH is a bicyclic peroxy radical which behaves similar to hydroxyalkyl peroxy radicals. After reaction with NO products decompose and react with O$_2$ yielding HO$_2$ very fast, so that the first reaction step becomes limiting to the conversion efficiency in the HO$_2$ detection cell. Therefore, the RO$_2$ radical species from benzene plus OH can be an interference for HO$_2$ measurements for conditions at which RO$_2$ radicals from alkene plus OH interfere.

6 Implication for atmospheric HO$_2$ concentration measurements by LIF

Investigation of relative detection sensitivities of the LIF instrument described in the previous section show that RO$_2$ can be a significant interference for HO$_2$ concentration measurements. Experiments indicate that a large fraction of RO$_2$ radicals from alkene plus OH reactions including isoprene and from aromatics plus OH reactions are detected for conditions, at which the instrument was operated during field campaigns in the past. Interferences from RO$_2$ radicals identified here (mostly β-hydroxyalkyl peroxy radicals), can be significantly reduced, if the NO concentration and/or the reaction time in the detection cell is decreased. Although the HO$_2$ detection sensitivity becomes smaller at the same time, operation of the instrument at lower NO concentration and with shorter reaction time is feasible. In this case, the HO$_2$ sensitivity is only reduced by a factor of four (Fig. 3), but the relative RO$_2$ sensitivity is smaller than 0.2 for most of RO$_2$ species studied here (Table 2). This value for the HO$_2$ sensitivity will be still sufficient for detecting HO$_2$ for a wide range of conditions in the atmosphere.

HO$_2$ measurements that we performed with our LIF instrument in past field campaigns and in simulation chamber experiments need to be revised, depending on the abundance and mix of RO$_2$ species present during the distinct campaigns. The interference by RO$_2$ is generally expected to be negligible for remote and marine environments, where methyl peroxy radicals are the dominant RO$_2$ species. However, significant interferences in HO$_2$ measurements are expected in the presence of high concentrations of alkenes and aromatics, as is typically found in urban and forested environments. In principle, speciated RO$_2$ measurements are required to correct for the interference, but such measurements do not exist. A detailed analysis of the consequences for past field measurements is beyond the scope of this paper and will be discussed elsewhere. For example, a significant impact of the interference is expected for the recently published HO$_x$ measurements performed during the PRIDE-PRD2006 campaign in the Pearl River Delta, China (Hofzumahaus et al., 2009). Model calculations suggest that the measured HO$_2$ concentrations contain an interference by RO$_2$ of at least 30 % during daytime, depending on the chemical mechanism used for the calculation of the RO$_2$ species (Lu et al., 2011). This also suggests that the unknown radical recycling, proposed by Hofzumahaus et al. (2009) to explain the observed OH, must be even larger, if the HO$_2$ concentrations are smaller than assumed before (Lu et al., 2011).

An LIF instrument similar to the one for HO$_2$ detection was recently developed for alternating measurement of HO$_x$ and RO$_x$ radicals (Fuchs et al., 2008). This instrument utilizes the conversion of RO$_2$ radicals to HO$_2$ as described above (Reactions R3, R4) in an additional conversion reactor that is mounted on top of a detection cell that is similar to the HO$_2$ detection cell characterized here. The sum of OH, HO$_2$

and RO$_2$ is converted to HO$_2$ in the conversion reactor in the RO$_x$-mode of the system. The RO$_2$ conversion efficiency in the reactor is mainly determined by the rate constant of the reaction of RO$_2$ with NO, so that effects described here, do not impact RO$_x$ measurements. However, since conditions were chosen for a high HO$_2$ conversion efficiency in the HO$_2$ detection cell downstream of the conversion reactor, HO$_2$ concentration measurements in the HO$_x$-mode of the instrument are affected by similar RO$_2$ interferences as described above. In the HO$_2$ measurement mode RO$_2$ radicals are not converted in the conversion reactor, but can be converted to OH in the HO$_2$ detection cell as shown above. Therefore, the instrument is not sufficiently capable of separating between HO$_2$ and RO$_2$ radicals from alkenes and aromatics. In the future, it is planned to install a separate HO$_2$ detection cell, which will be operated at optimized conditions (low NO concentration and shorter reaction time). This will allow separating HO$_2$ and RO$_2$ radical concentrations by subtracting the signals of the RO$_x$- and HO$_x$-channel of the instrument. HO$_2$ comparison measurements of ROxLIF with measurements by MIESR in the past (Fuchs et al., 2009) is expected to be unaffected by interferences from RO$_2$, because only methyl peroxy radicals and ethyl peroxy radicals, which are not efficiently converted in the HO$_2$ detection cell, were involved. This expectation is consistent with the good correlation and absolute agreement between HO$_2$ and RO$_2$ concentration measurements of both instruments observed for the two techniques.

Although NO concentrations and reaction times in the detection cell are different for other LIF instruments, it is likely that these instruments also suffer from the interferences discovered here. All LIF-instruments make use of the conversion of HO$_2$ via reaction with NO reach HO$_2$ conversion efficiencies that are greater than 0.9 (Heard and Pilling, 2003). As shown above, the HO$_2$ conversion efficiency is closely connected to the RO$_2$ conversion efficiency for RO$_2$ species from alkene- and aromatic-precursors and can reach similar values for large NO concentrations. After publication of the discussion paper of this study two groups (Max Planck Institute for Chemistry, MPIC, and University of Leeds) reported in Interactive Comments to the paper that their LIF instruments suffer from the same interference observed here, if instruments are operated at conditions with a high HO$_2$ conversion efficiency. They also investigated RO$_2$ radicals from larger alkanes ($>$C$_3$) that were not investigated here and found an interference.

HO$_2$ concentration measurements of three LIF instruments were compared during the HOxCOMP campaign in 2005 (Fuchs et al., 2010). Measurements were partly conducted in ambient air and partly at the atmosphere simulation chamber SAPHIR. Since the measurement place was influenced by biogenic emissions, most likely RO$_2$ radicals from isoprene and its reaction products were present during ambient air sampling and may have corrupted HO$_2$ concentrations that were reported for the three instruments. However, the

interference would likely appear in a difference in the slope from unity in the correlation plot rather than in an offset for two reasons: (1) HO$_2$ and RO$_2$ concentrations are often highly correlated (Mihelcic et al., 2003), (2) measurements of all instruments were most likely affected in a similar way. Thus, the interference would not be distinguishable from calibration errors. This is also the case for those experiments in SAPHIR during which RO$_2$ radicals were produced. It is possible that some of the day-to-day variability observed in the slope of the correlation may have been caused by interferences from RO$_2$ radicals. However, half of the experiments in SAPHIR were conducted without the addition of organic compounds. Therefore, it is likely that major results of this campaign are not related to an interference from RO$_2$ radicals.

7 Summary and conclusions

HO$_2$ concentration measurements are widely accomplished by chemical conversion of HO$_2$ to OH including reaction with NO and subsequent detection of OH by laser-induced fluorescence. RO$_2$ radicals can be converted to OH via a similar radical reaction sequence including reaction with NO, so that they are potential interferences for HO$_2$ measurements. It was believed that this reaction path does not play a role for LIF instruments. Here, RO$_2$ detection sensitivities relative to that for HO$_2$ were measured for RO$_2$ radicals from various organic precursors such as alkanes, alkenes including isoprene and aromatics. They were produced by the reaction of VOCs with OH in a radical source that produces OH and HO$_2$ by water photolysis. The ratio of OH and HO$_2$ concentrations in the radical source were determined in a separate experiment, in order to avoid uncertainties from potential discrepancies of the ratio from unity. Major results of these investigations are:

– The ratio of HO$_2$ to the sum of HO$_2$ and OH concentrations produced by water photolysis at 185 mm in air is 0.50 ± 0.02.

– The interference of HO$_2$ measurements from RO$_2$ produced by the reaction of OH with small alkanes via H-atom abstraction tested here (methane and ethane) is within the range of a few percent for the LIF instrument operated at conditions used in field campaigns in the past in agreement with results reported from other groups.

– The interference from RO$_2$ from OH plus alkenes or aromatics (OH-addition) is larger than 0.8 for the LIF instrument operated with these conditions.

– Interferences from RO$_2$ radicals produced by the reaction of isoprene and its oxidation products, MVK and MACR, with OH are 0.8 and 0.6, respectively, for the LIF instrument operated with these conditions.

– The reaction of RO$_2$ with NO limits the conversion efficiency for interfering RO$_2$ radical species in contrast to assumptions made in the past that the reaction of alkoxy radicals with O$_2$ suppresses the conversion (Holland et al., 2003). This is due to the fast reaction of β-hydroxyalkoxy radicals with O$_2$.

– Interferences from these RO$_2$ species can be significantly reduced (<0.2), if the reaction time and/or the NO concentration in the detection cell is reduced at the expense of a reduced HO$_2$ detection sensitivity.

Consequently, HO$_2$ concentration measurements from previous field campaigns during which this LIF instrument was deployed give rather the sum of HO$_2$ and some fraction of RO$_2$ than HO$_2$ alone. Generally, the interference by RO$_2$ radicals would be small in clean remote environments, when small alkanes dominate the OH reactivity, but would be most likely larger in polluted environments. This is also the case for areas that have large biogenic emissions, because RO$_2$ radicals from isoprene and its oxidation products are efficiently converted in the detection cell. The impact of interferences from RO$_2$ is highest, if the oxidation rate of pollutants such as alkenes including isoprene is high (high VOC and OH concentrations) but NO concentrations are small as found e.g. during the PRIDE-PRD2006 campaign (Lu et al., 2011). For this campaign, model calculations suggest that the measured HO$_2$ concentrations contain an interference by RO$_2$ of at least 30 % during daytime. The unknown radical recycling, proposed by Hofzumahaus et al. (2009) to explain the observed OH, however, must be even larger, if the OH source from HO$_2$ is smaller than assumed before.

Results of investigations done here implicate that the detection of HO$_2$ via chemical conversion with NO and subsequent detection of OH needs to be revisited. Running the LIF instrument at much lower NO concentration and/or shorter reaction time for HO$_2$ to OH conversion will provide a significantly improved suppression of interferences from RO$_2$ (less than 0.2). Although the HO$_2$ sensitivity of the instrument will be reduced at the same time, this should allow useful studies of the atmospheric chemistry at most tropospheric conditions. Further characterization of interferences for a wider range of RO$_2$ species and redesign of the instrument may be required, in order to minimize interferences from RO$_2$ radicals.

Edited by: M. D. Andrés Hernóndez

References

Andrés-Hernández, M. D., Stone, D., Brookes, D. M., Commane, R., Reeves, C. E., Huntrieser, H., Heard, D. E., Monks, P. S., Burrows, J. P., Schlager, H., Kartal, D., Evans, M. J., Floquet, C. F. A., Ingham, T., Methven, J., and Parker, A. E.: Peroxy radical partitioning during the AMMA radical intercomparison exercise, Atmos. Chem. Phys., 10, 10621–10638, doi:10.5194/acp-10-10621-2010, 2010.

Aschmann, S. M., Chew, A. A., Arey, J., and Atkinson, R.: Products of the gas-phase reaction of OH radicals with cyclohexane: reactions of the cyclohexoxy radical, J. Phys. Chem. A, 101, 8042–8048, doi:10.1021/jp971869f, 1997.

Aschmutat, U., Hessling, M., Holland, F., and Hofzumahaus, A.: A tunable source of hydroxyl (OH) and hydroperoxy (HO$_2$) radicals: in the range between 10^6 and 10^9 cm^{-3}, Physicochemical behaviour of atmospheric pollutants, European Commission, Brussels, 1994.

Atkinson, R.: Gase-phase tropospheric chemistry of volatile organic compounds: 1. Alkanes and alkenes, J. Phys. Chem. Ref. Data, 26, 217–290, 1997a.

Atkinson, R.: Atmospheric reactions of alkoxy and β-hydroxyalkoxy radicals, Int. J. Chem. Kinet., 29, 99–111, 1997b.

Atkinson, R. and Arey, J.: Atmospheric degradation of volatile organic compounds, Chem. Rev., 103, 4605–4638, doi:10.1021/cr0206420, 2003.

Bajeh, M. A., Goldfield, E. M., Hanf, A., Kappel, C., Meijer, A. J. H. M., Volpp, H.-R., and Wolfrum, J.: Dynamics of the H + O$_2$ → O + OH chain-branching reaction: accurate quantum mechanical and experimental absolute reaction cross sections, J. Phys. Chem. A, 105, 3359–3364, doi:10.1021/jp0036137, 2001.

Bloss, C., Wagner, V., Bonzanini, A., Jenkin, M. E., Wirtz, K., Martin-Reviejo, M., and Pilling, M. J.: Evaluation of detailed aromatic mechanisms (MCMv3 and MCMv3.1) against environmental chamber data, Atmos. Chem. Phys., 5, 623–639, doi:10.5194/acp-5-623-2005, 2005a.

Bloss, C., Wagner, V., Jenkin, M. E., Volkamer, R., Bloss, W. J., Lee, J. D., Heard, D. E., Wirtz, K., Martin-Reviejo, M., Rea, G., Wenger, J. C., and Pilling, M. J.: Development of a detailed chemical mechanism (MCMv3.1) for the atmospheric oxidation of aromatic hydrocarbons, Atmos. Chem. Phys., 5, 641–664, doi:10.5194/acp-5-641-2005, 2005b.

Bohn, B. and Zetzsch, C.: Gas-phase reaction of the OH-benzene adduct with O$_2$: reversibility and secondary formation of HO$_2$, Phys. Chem. Chem. Phys., 1, 5097–5107, 1999.

Burkert, J., Hernández, M. D. A., Stöbener, D., Weissenmayer, M., and Kraus, A.: Peroxy radical and related trace gas measurements in the boundary layer above the Atlantic Ocean, J. Geophys. Res., 106, 5457–5477, 2001.

Cantrell, C. A., Stedman, D. H., and Wendel, G. J.: Measurement of atmospheric peroxy radicals by chemical amplification, Anal. Chem., 56, 1496–1502, 1984.

Cantrell, C. A., Zimmer, A., and Tyndall, G. S.: Absorption cross sections for water vapor from 183 to 193 nm, Geophys. Res. Lett., 24, 2195–2198, 1997.

Clemitshaw, K. C., Carpenter, L. J., and St, A. P.: A calibrated peroxy radical chemical amplifier for ground-based tropospheric measuerments, J. Geophys. Res., 102, 25405–25416, 1997.

Creasey, D. J., Heard, D. E., Pilling, M. J., Whitaker, B. J., Berzins, M., and Fairlie, R.: Visualisation of a supersonic free-jet expansion using laser-induced fluorescence spectroscopy: Application of measurement of rate constants at ultralow temperatures, Appl. Phys. B., 65, 375–391, 1997.

Creasey, D. J., Heard, D. E., and Lee, J. D.: Absorption cross section measurements of water vapour and oxygen at 185 nm, Implications for the calibration of field instruments to measure OH, HO$_2$ and RO$_2$ radicals, Geophys. Res. Lett., 27, 1651–1654, doi:10.1029/1999GL011014, 2000.

Creasey, D. J., Heard, D. E., and Lee, J. D.: Eastern Atlantic Spring Experiment 1997 (EASE97) 1. Measurements of OH and HO$_2$ concentrations at Mace Head, Ireland, J. Geophys. Res., 107, 4091, doi:10.1029/2001jd000892, 2002.

Creasey, D. J., Evans, G. E., Heard, D. E., and Lee, J. D.: Measurements of OH and HO$_2$ concentrations in the Southern Ocean marine boundary layer, J. Geophys. Res., 108, 4475, doi:10.1029/2002JD003206, 2003.

da Silva, G., Graham, C., and Wang, Z.-F.: Unimolecular β-hydroxyperoxy radical decomposition with OH recycling in the photochemical oxidation of isoprene, Environ Sci. Technol., 44, 250–256, doi:10.1021/es900924d, 2010.

Demers, R., Collin, G. J., and Gagnon-Deslauriers, H.: Photolyse de l'isopréne gazeux entre son seuil d'absorption (ca. 255 nm) et 147.0 nm, Can. J. Chem., 56, 1864–1870, doi:10.1139/v78-303, 1978.

Dlugi, R., Berger, M., Zelger, M., Hofzumahaus, A., Siese, M., Holland, F., Wisthaler, A., Grabmer, W., Hansel, A., Koppmann, R., Kramm, G., Möllmann-Coers, M., and Knaps, A.: Turbulent exchange and segregation of HO$_x$ radicals and volatile organic compounds above a deciduous forest, Atmos. Chem. Phys., 10, 6215–6235, doi:10.5194/acp-10-6215-2010, 2010.

Edwards, G. D., Cantrell, C. A., Stephens, S., Hil, B., Goyea, O., Shetter, R. E., Mauldin, R. L., Kosciuch, E., Tanner, D. J., and Eisele, F. L.: Chemical ionization mass spectrometer instrument for the measurement of tropospheric HO$_2$ and RO$_2$, Anal. Chem., 75, 5318–5327, doi:10.1021/ac034402b, 2003.

Engel, V., Staemmler, V., Vander Wal, R. L., Crim, F. F., Sension, R. J., Hudson, B., Andresen, P., Hennig, S., Weide, K., and Schinke, R.: Photodissociation of water in the first absorption band: a prototype for dissociation on a repulsive potential energy surface, J. Phys. Chem., 96, 3201–3213, doi:10.1021/j100187a007, 1992.

Fan, J. and Zhang, R.: Atmospheric oxidation mechanism of isoprene, Environ. Chem., 1, 140–149, doi:10.1071/EN04045, 2004.

Finlayson-Pitts, B. J. and Pitts Jr., J. N.: Chemistry of the Upper and Lower Atmosphere, Academic Press, San Diego, 2000.

Fuchs, H., Hofzumahaus, A., and Holland, F.: Measurement of tropospheric RO$_2$ and HO$_2$ radicals by a laser-induced fluorescence instrument, Rev. Sci. Instrum., 79, 084104, doi:10.1063/1.2968712, 2008.

Fuchs, H., Brauers, T., Häseler, R., Holland, F., Mihelcic, D., Müsgen, P., Rohrer, F., Wegener, R., and Hofzumahaus, A.: Intercomparison of peroxy radical measurements obtained at atmospheric conditions by laser-induced fluorescence and electron spin resonance spectroscopy, Atmos. Meas. Tech., 2, 55–64, doi:10.5194/amt-2-55-2009, 2009.

Fuchs, H., Brauers, T., Dorn, H.-P., Harder, H., Häseler, R., Hofzumahaus, A., Holland, F., Kanaya, Y., Kajii, Y., Kubistin, D., Lou, S., Martinez, M., Miyamoto, K., Nishida, S., Rudolf, M., Schlosser, E., Wahner, A., Yoshino, A., and Schurath, U.: Technical Note: Formal blind intercomparison of HO_2 measurements in the atmosphere simulation chamber SAPHIR during the HOxComp campaign, Atmos. Chem. Phys., 10, 12233–12250, doi:10.5194/acp-10-12233-2010, 2010.

Geyer, A., Bächmann, K., Hofzumahaus, A., Holland, F., Konrad, S., Klüpfel, T., Pätz, H. W., Schäfer, J., and Platt, U.: Nighttime formation of peroxy and hydroxyl radicals during the BERLIOZ campaign: observations and modeling studies, J. Geophys. Res., 108, 8249, doi:10.1029/2001JD000656, 2003.

Ghosh, B., Bugarin, A., Connell, B. T., and North, S. W.: Isomer-selective study of the OH-initiated oxidation of isoprene in the presence of O_2 and NO: 2. The major OH addition channel, J. Phys. Chem. A, 114, 2553–2560, doi:10.1021/jp909052t, 2010.

Giroux, L., Back, M. H., and Back, R. A.: The photolysis of ethylene at 193 nm, Can. J. Chem., 67, 1166–1173, doi:10.1139/v89-176, 1989.

Green, T. J., Reeves, C. E., Fleming, Z. L., Brough, N., Rickard, A. R., Bandy, B. J., Monks, P. S., and Penkett, S. A.: An improved dual channel PERCA instrument for atmospheric measurements of peroxy radicals, J. Environ. Monitor., 8, 530–536, 2006.

Greenwald, E. E., Ghosh, B., Anderson, K. C., Dooley, K. S., Zou, P., Selby, T., Osborn, D. L., Meloni, G., Taatjes, C. A., Goulay, F., and North, S. W.: Isomer-selective study of the OH initiated oxidation of isoprene in the presence of O_2 and NO, I. The minor inner OH-addition channel, J. Phys. Chem. A, 114, 904–912, doi:10.1021/jp908543a, 2010.

Hanke, M., Uecker, J., Reiner, T., and Arnold, F.: Atmospheric peroxy radicals: ROXMAS, a new mass-spectrometric methodology for the speciated measurements of HO_2 and ΣRO_2 and first results, Int. J. Mass. Spectrom., 213, 91–99, 2002.

Hard, T. M., O'Brian, R. J., Chan, C. Y., and Mehrabzadeh, A. A.: Tropospheric free radical determination by FAGE, Environ. Sci. Technol., 18, 768–777, 1984.

Hastie, D. R., Weissenmayer, M., Burrows, J. P., and Harris, G. W.: Calibrated chemical amplifier for atmospheric RO_x measurements, Anal. Chem., 63, 2048–2057, 1991.

Heard, D. E. and Pilling, M. J.: Measurement of OH and HO_2 in the troposphere, Chem. Rev., 103, 5163–5198, doi:10.1021/cr020522s, 2003.

Heard, D. E. and Henderson, D. A.: Quenching of $OH(A^2\Sigma^+, \nu' = 0)$ several collision partners between 200 and 344 K. Cross-section measurements and model comparisons, Phys. Chem. Chem. Phys., 2, 67–72, 2000.

Hofzumahaus, A., Aschmutat, U., Heßling, M., Holland, F., and Ehhalt, D. H.: The measurement of tropospheric OH radicals by laser-induced fluorescence spectroscopy during POPCORN field campaign, Geophys. Res. Lett., 23, 2541–2544, 1996.

Hofzumahaus, A., Rohrer, F., Lu, K., Bohn, B., Brauers, T., Chang, C.-C., Fuchs, H., Holland, F., Kita, K., Kondo, Y., Li, X., Lou, S., Shao, M., Zeng, L., Wahner, A., and Zhang, Y.: Amplified trace gas removal in the troposphere, Science, 324, 1702–1704, doi:10.1126/science.1164566, 2009.

Holland, F., Heßling, M., and Hofzumahaus, A.: In situ measurement of tropospheric OH radicals by laser-induced fluorescence – a description of the KFA instrument, J. Atmos. Sci., 52, 3393–3401, 1995.

Holland, F., Hofzumahaus, A., Schäfer, J., Kraus, A., and Pätz, H. W.: Measurements of OH and HO_2 radical concentrations and photolysis frequencies during BERLIOZ, J. Geophys. Res., 108, 8246, doi:10.1029/2001JD001393, 2003.

Hornbrook, R. S., Crawford, J. H., Edwards, G. D., Goyea, O., Mauldin III, R. L., Olson, J. S., and Cantrell, C. A.: Measurements of tropospheric HO_2 and RO_2 by oxygen dilution modulation and chemical ionization mass spectrometry, Atmos. Meas. Tech., 4, 735–756, doi:10.5194/amt-4-735-2011, 2011.

Jenkin, M. E., Saunders, S. M., Wagner, V., and Pilling, M. J.: Protocol for the development of the Master Chemical Mechanism, MCM v3 (Part B): tropospheric degradation of aromatic volatile organic compounds, Atmos. Chem. Phys., 3, 181–193, doi:10.5194/acp-3-181-2003, 2003.

Kanaya, Y., Sadanaga, Y., Nakamura, K., and Akimoto, H.: Development of a ground-based LIF instrument for measuring HO_x radicals: instrumentation and calibration, J. Atmos. Chem., 38, 73–110, 2001.

Kanaya, Y., Cao, R., Akimoto, H., Fukuda, M., Komazaki, Y., Yokouchi, Y., Koike, M., Tanimoto, H., Takegawa, N., and Kondo, Y.: Urban photochemistry in central Tokyo: 1. observed and modeled OH and HO_2 radical concentrations during the winter and summer 2004, J. Geophys. Res., 112, D21312, doi:10.1029/2007JD008670, 2007.

Kleffmann, J., Gavriloaiei, T., Hofzumahaus, A., Holland, F., Koppmann, R., Rupp, L., Schlosser, E., Siese, M., and Wahner, A.: Daytime formation of nitrous acid: a major source of OH radicals in a forest, Geophys. Res. Lett., 32, L05818, doi:10.1029/2005GL022524, 2005.

Lelieveld, J., Butler, T. M., Crowley, J. N., Dillon, T. J., Fischer, H., Ganzeveld, L., Harder, H., Lawrence, M. G., Martinez, M., Taraborrelli, D., and Williams, J.: Atmospheric oxidation capacity sustained by a tropical forest, Nature, 452, 737–740, doi:10.1038/nature06870, 2008.

Lu, K. D., Rohrer, F., Holland, F., Fuchs, H., Bohn, B., Brauers, T., Chang, C. C., Häseler, R., Hu, M., Kita, K., Kondo, Y., Li, X., Lou, S. R., Nehr, S., Shao, M., Zeng, L. M., Wahner, A., Zhang, Y. H., and Hofzumahaus, A.: Observation and modelling of OH and HO_2 concentrations in the Pearl River Delta 2006: a missing OH source in a VOC rich atmosphere, Atmos. Chem. Phys. Discuss., 11, 11311–11378, doi:10.5194/acpd-11-11311-2011, 2011.

Mather, J. H., Stevens, P. S., and Brune, W. H.: OH and HO_2 measurements using laser-induced fluorescence, J. Geophys. Res., 102, 6427–6436, 1997.

Mihelcic, D., Müsgen, P., and Ehhalt, D. H.: An improved method of measuring tropospheric NO_2 and RO_2 by matrix isolation and electron spin resonance, J. Atmos. Chem., 3, 341–361, 1985.

Mihelcic, D., Volz-Thomas, A., Pätz, H. W., Kley, D., and Mihelcic, M.: Numerical analysis of ESR spectra from atmospheric samples, J. Atmos. Chem., 11, 271–297, 1990.

Mihelcic, D., Holland, F., Hofzumahaus, A., Hoppe, L., Müsgen, P., Pätz, H. W., and Moortgat, G. K.: Peroxy radicals during BERLIOZ at Pabstthum: measurements, radical budgets and ozone production, J. Geophys. Res., 108, 9–1,

doi:10.1029/2001JD001014, 2003.

Mihele, C. M. and Hastie, D. R.: The sensitivity of the radical amplifier to ambient water vapor, Geophys. Res. Lett., 25, 1911–1913, 1998.

Mihele, C. M. and Hastie, D. R.: Optimized operation and calibration procedures for radical amplifyer-type detectors, J. Atmos. Ocean. Tech., 17, 788–794, 2000.

Monks, P. S.: Gas-phase radical chemistry in the troposphere, Chem. Soc. Rev., 34, 376–395, doi:10.1039/b307982c, 2005.

Nehr, S., Bohn, B., Fuchs, H., Hofzumahaus, A., and Wahner, A.: HO$_2$ formation from the OH + benzene reaction in the presence of O$_2$, Phys. Chem. Chem. Phys., 13, 10699–10708, doi:10.1039/C1CP20334G, 2011,

Orlando, J. J., Tyndall, G. S., Bilde, M., Ferronato, C., Wallington, T. J., Vereecken, L., and Peeters, J.: Laboratory and theoretical study of the oxy radicals in the OH- and Cl-initiated oxidation of ethene, J. Phys. Chem. A, 102, 8116–8123, doi:10.1021/jp981937d, 1998.

Orlando, J. J., Tyndall, G. S., and Paulson, S. E.: Mechanism of the OH-initiated oxidation of methacrolein, Geophys. Res. Lett., 26, 2191–2194, doi:10.1029/1999gl900453, 1999.

Orlando, J. J., Iraci, L. T., and Tyndall, G. S.: Chemistry of the cyclopentoxy and cyclohexoxy radicals at sub-ambient temperatures, J. Phys. Chem. A, 104, 5072–5079, doi:10.1021/jp0002648, 2000.

Orlando, J. J., Tyndall, G. S., and Wallington, T. J.: The atmospheric chemistry of alkoxy radicals, Chem. Rev., 103, 4657–4689, doi:10.1021/cr020527p, 2003.

Peeters, J. and Muller, J.-F.: HO$_x$ radical regeneration in isoprene oxidation via peroxy radical isomerisations, II: experimental evidence and global impact, Phys. Chem. Chem. Phys., 12, 14227–14235, doi:10.1039/C0CP00811G, 2010.

Peeters, J., Nguyen, T. L., and Vereecken, L.: HO$_x$ radical regeneration in the oxidation of isoprene, Phys. Chem. Chem. Phys., 11, 5935–5939, doi:10.1039/b908511d, 2009.

Platt, U., Alicke, B., Dubois, R., Geyer, A., Hofzumahaus, A., Holland, F., Martinez, M., and Stutz, J.: Free radicals and fast photochemistry during BERLIOZ, J. Atmos. Chem., 42, 359–394, 2002.

Qi, B., Takami, A., and Hatakeyama, S.: A calibration method for measurement of small alkyl organic peroxy radicals by chemical amplifier, Anal. Sci., 22, 1091–1093, 2006.

Ren, X., Edwards, G. D., Cantrell, C. A., Lesher, R. L., Metcalf, A. R., Shirley, T., and Brune, W. H.: Intercomparison of peroxy radical measurements at a rural site using laser-induced fluorescence and peroxy radical chemical ionization mass spectrometer (PerCIMS) techniques, J. Geophys. Res., 108, 4605, doi:10.1029/2003JD003644, 2003.

Ren, X., Harder, H., Martinez, M., Falona, I. C., Tan, D., Lesher, R. L., Carlo, P. D., Simpas, J. B., and Brune, W. H.: Interference testing for atmospheric HO$_x$ measurements by laser-induced fluorescence, J. Atmos. Chem., 47, 169–190, 2004.

Ren, X., Olson, J. R., Crawford, J. H., Brune, W. H., Mao, J., Long, R. B., Chen, Z., Chen, G., Avery, M. A., Sachse, G. W., Barrick, J. D., Diskin, G. S., Huey, L. G., Fried, A., Cohen, R. C., Heikes, B., Wennberg, P. O., Singh, H. B., Blake, D. R., and Shetter, R. E.: HO$_x$ chemistry during INTEX-A 2004: observation, model calculation, and comparison with previous studies, J. Geophys. Res., 113, D05310, doi:10.1029/2007JD009166, 2008.

Sadanaga, Y., Yoshino, A., Watanaba, K., Yoshioka, A., Wakazono, Y., Kanaya, Y., and Kajii, Y.: Development of a measurement system of peroxy radicals using a chemical amplification/laser-induced fluorescence technique, Rev. Sci. Instrum., 75, 864–872, doi:10.1063/1.1666985, 2004.

Saunders, S. M., Jenkin, M. E., Derwent, R. G., and Pilling, M. J.: Protocol for the development of the Master Chemical Mechanism, MCM v3 (Part A): tropospheric degradation of non-aromatic volatile organic compounds, Atmos. Chem. Phys., 3, 161–180, doi:10.5194/acp-3-161-2003, 2003.

Schultz, M., Heitlinger, M., Mihelcic, D., and Volz-Thomas, A.: Calibration source for peroxy radicals with built-in actinometry using H$_2$O and O$_2$ photolysis at 185 nm, J. Geophys. Res., 100, 18811–18816, 1995.

Stevens, P. S., Mather, J. H., and Brune, W. H.: Measurement of tropospheric OH and HO$_2$ by laser-induced fluorescence at low pressure, J. Geophys. Res., 99, 3543–3557, 1994.

Tuazon, E. C. and Atkinson, R.: A product study of the gas-phase reaction of methyl vinyl ketone with the OH radical in the presence of NO$_x$, Int. J. Chem. Kinet., 21, 1141–1152, doi:10.1002/kin.550211207, 1989.

Tuazon, E. C. and Atkinson, R.: A product study of the gas-phase reaction of methacrolein with the OH radical in the presence of NO$_x$, Int. J. Chem. Kinet., 22, 591–602, doi:10.1002/kin.550220604, 1990.

Vereecken, L., Peeters, J., Orlando, J. J., Tyndall, G. S., and Ferronato, C.: Decomposition of β-hydroxypropoxy radicals in the OH-initiated oxidation of propene, A theoretical and experimental study, J. Phys. Chem. A, 103, 4693–4702, doi:10.1021/jp990046i, 1999.

Volkamer, R., Klotz, B., Barnes, I., Imamura, T., Wirtz, K., Washida, N., Becker, K. H., and Platt, U.: OH-initiated oxidation of benzene Part I, Phenol formation under atmospheric conditions, Phys. Chem. Chem. Phys., 4, 1598–1610, doi:10.1039/b108747a, 2002.

Washida, N., Mori, Y., and Tanaka, I.: Quantum yield of ozone formation from photolysis of the oxygen molecule at 1849 and 1931 A, J. Chem. Phys., 54, 1119–1122, doi:10.1063/1.1674946, 1971.

Weber, M.: Entwicklung und Einsatz eines Instrumentes zur Bestimmung der Konzentration von HO$_2$-Radikalen in der Troposphäre, Ph.D. thesis, Universitaet Köln, Köln, 1998.

Zhang, D. H., Collins, M. A., and Lee, S.-Y.: First-principle theory for the H + H$_2$O, D$_2$O reactions, Science, 290, 961–963, 2000.

Zhang, J., Dransfield, T., and Donahue, N. M.: On the mechanism for nitrate formation via the peroxy radical + NO reaction, J. Phys. Chem. A, 108, 9082–9095, doi:10.1021/jp048096x, 2004.